

Universal versus Material-Dependent Two-Gap Behaviors of the High- T_c Cuprate Superconductors: Angle-Resolved Photoemission Study of $\text{La}_{2-x}\text{Sr}_x\text{CuO}_4$

T. Yoshida,¹ M. Hashimoto,¹ S. Ideta,¹ A. Fujimori,¹ K. Tanaka,² N. Mannella,² Z. Hussain,³ Z.-X. Shen,² M. Kubota,⁴ K. Ono,⁴ Seiki Komiya,⁵ Yoichi Ando,⁶ H. Eisaki,⁷ and S. Uchida¹

¹*Department of Physics, University of Tokyo, Bunkyo-ku, Tokyo 113-0033, Japan*

²*Department of Applied Physics and Stanford Synchrotron Radiation Laboratory, Stanford University, Stanford, California 94305, USA*

³*Advanced Light Source, Lawrence Berkeley National Lab, Berkeley, California 94720, USA*

⁴*Photon Factory, Institute of Materials Structure Science, KEK, Tsukuba, Ibaraki 305-0801, Japan*

⁵*Central Research Institute of Electric Power Industry, Komae, Tokyo 201-8511, Japan*

⁶*Institute of Scientific and Industrial Research, Osaka University, Ibaraki, Osaka 567-0047, Japan*

⁷*National Institute of Advanced Industrial Science and Technology, Tsukuba 305-8568, Japan*

(Received 30 November 2008; published 16 July 2009)

We have investigated the doping and temperature dependences of the pseudogap and superconducting gap in the single-layer cuprate $\text{La}_{2-x}\text{Sr}_x\text{CuO}_4$ by angle-resolved photoemission spectroscopy. The results clearly exhibit two distinct energy and temperature scales, namely, the gap around $(\pi, 0)$ of magnitude Δ^* and the gap around the node characterized by the d -wave order parameter Δ_0 . In comparison with Bi2212 having higher T_c 's, Δ_0 is smaller, while Δ^* and T^* are similar. This result suggests that Δ^* and T^* are approximately material-independent properties of a single CuO_2 plane, in contrast to the material-dependent Δ_0 , representing the pairing strength.

DOI: 10.1103/PhysRevLett.103.037004

PACS numbers: 74.25.Jb, 71.18.+y, 74.72.Dn, 79.60.-i

One of the central issues in the studies of high- T_c cuprates is whether the pseudogap is related to the superconductivity or a phenomenon distinct from superconductivity. In the former scenario, possible origins of the pseudogap are preformed Cooper pairs lacking phase coherence [1] or superconducting fluctuations [2]. In the latter scenario, the pseudogap is due to a competing order such as spin density wave, charge density wave, d -density wave [3], etc. It has been well known that the pseudogap in the antinodal $\sim (\pi, 0)$ region increases with underdoping as observed by angle-resolved photoemission spectroscopy (ARPES) [4] and tunneling spectroscopy [5]. However, the energy gap measured by Andreev reflection [6], penetration depth [7], and Raman experiments in B_{2g} -geometry [8,9], which is directly associated with superconductivity, exhibits the opposite trend, that is, the gap decreases with underdoping, suggesting a different origin of the superconducting gap from the antinodal gap.

A recent ARPES study of deeply underdoped $\text{Bi}_2\text{Sr}_2\text{Ca}_{1-x}\text{Y}_x\text{Cu}_2\text{O}_8$ (Bi2212) has revealed the presence of two distinct energy gaps between the nodal and antinodal region [10,11]. A similar two-gap behavior has been observed in the optimally doped single-layer cuprate $\text{Bi}_2\text{Sr}_2\text{CuO}_{6+\delta}$ (Bi2201) [12,13] and $\text{La}_{2-x}\text{Sr}_x\text{CuO}_4$ (LSCO) [14,15]. On the other hand, attempts have been made to understand the pseudogap within a single d -wave energy gap [16–19]. From the measurement of the Fermi arc length, Kanigel *et al.* [18] has proposed that the $T = 0$ ground state of the pseudogap state is a nodal liquid which has a single $d_{x^2-y^2}$ gap. In such a single gap picture,

preformed Cooper pairs are the most likely origin of the pseudogap.

Since the doping and temperature dependences of the energy gap would reveal the entangled two-gap behavior, we have investigated the energy gap of LSCO by ARPES as a function of doping and temperature. In the present work, the momentum dependence of the gap clearly exhibits two-gap behavior as in the previous studies [10–15]: the pseudogap Δ^* in the antinodal region and the d -wave-like gap Δ_0 around the node. Furthermore, from comparison with those on Bi2212, we have found that the magnitude of the Δ^* and the pseudogap temperature T^* is not appreciably material-dependent, suggesting that the pseudogap is a property of a single CuO_2 plane. On the other hand, the magnitude of the Δ_0 , which is proportional to the superconducting gap, is strongly material dependent (CuO_2 layer number dependent) like T_c .

High-quality single crystals of LSCO ($x = 0.03, 0.07, 0.15$) were grown by the traveling-solvent floating-zone method. The critical temperatures (T_c 's) of the $x = 0.07, 0.15$ samples were 14 and 39 K, respectively, and the $x = 0.03$ samples were nonsuperconducting. The ARPES measurements were carried out at BL10.0.1 of Advanced Light Source (ALS) and at BL-28A of Photon Factory (PF) using incident photons of linearly polarized 55.5 eV and circularly polarized 55 eV, respectively. SCIENTA R4000 and SES-2002 analyzer were used at ALS and PF, respectively, with the total energy resolution of ~ 20 meV and momentum resolution of $\sim 0.02\pi/a$, where $a = 3.8$ Å is the lattice constant. The samples were cleaved *in situ* and

measurements were performed from 20 to 155 K. In the measurements at ALS, the electric field vector \mathbf{E} of the incident photons lies in the CuO_2 plane, rotated by 45° from the Cu-O bond direction, which enhances the dipole matrix elements in the nodal region [20].

Figure 1 illustrates that the quasiparticle (QP) band dispersions are determined by momentum distribution curve (MDC) peak positions. Here, the Fermi momentum k_F is defined by the momentum where the QP dispersion crosses the E_F . To quantify the energy gap size, the leading edge midpoints (LEM's) of the energy distribution curves (EDC's) at k_F shall be used in the present analysis. As shown in Figs. 1(d), 1(e), and 1(f), the LEM's at k_F are shifted toward higher binding energies in going from the node to the antinode, indicating an anisotropic gap opening.

The gap sizes have been evaluated from the shift (Δ_{LEM}) of the LEM of EDC's relative to the node. The angular dependence of the gap for each doping is plotted as a function of the d -wave parameter $|\cos(k_x a) - \cos(k_y a)|/2$ in Fig. 2(a). These plots do not obey the simple straight line expected for the pure d -wave order parameter but has a kink at $|\cos(k_x a) - \cos(k_y a)|/2 \cong 0.7$ – 0.9 . Interestingly, the kink occurs near the antiferromagnetic Brillouin-zone

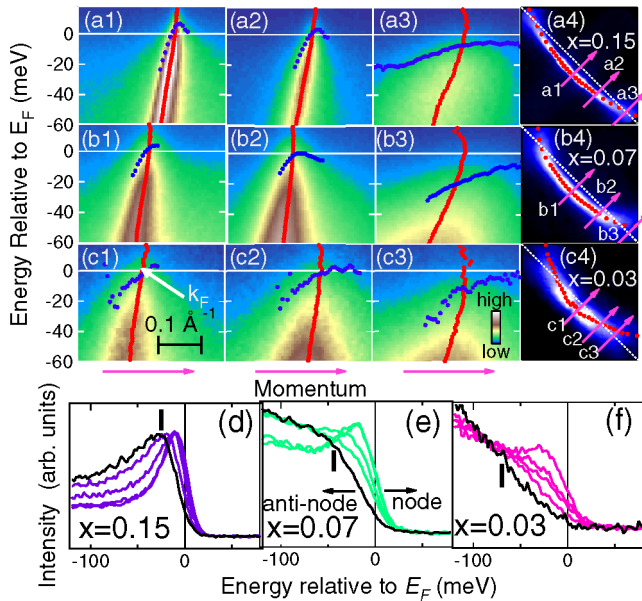


FIG. 1 (color online). ARPES intensity plot of $\text{La}_{2-x}\text{Sr}_x\text{CuO}_4$ (LSCO). (a1)–(a3), (b1)–(b3), and (c1)–(c3): Band image plots in energy-momentum (E - k) space for $x = 0.15$, 0.07 and 0.03 , respectively. Energy dispersions determined by MDC's peaks and leading edge midpoints (LEM) are shown by red dots and blue dots, respectively. (a4), (b4), and (c4): Spectral weight mapping at E_F in momentum space for each doping level. Red dots indicate Fermi momenta k_F . White dotted lines indicate the antiferromagnetic Brillouin zone (AMF BZ). (d)–(f): EDC's at k_F for each doping level. Black lines correspond to antinodal EDC's and vertical bars represent energy position of the antinode gap.

(AFM BZ) boundary but not exactly on it, as shown by vertical arrows. Qualitatively the same results have been obtained for the single-layer cuprates Bi2201 [12] and underdoped Bi2212 [10,11]. Note that the gaps for $x = 0.07$ near the node are almost closed above T_c ($=14$ K), but d -wave-like gap opens below T_c as shown in the inset.

In order to discuss the character of the energy gaps, we define two distinct energy scales Δ^* and Δ_0 : Δ^* from Δ_{LEM} closest to $|\cos(k_x a) - \cos(k_y a)|/2 = 1$ and Δ_0 from the extrapolation of the linear dependence near the node toward $|\cos(k_x a) - \cos(k_y a)|/2 = 1$, as indicated in panel (a). Since the Δ_{LEM} is affected by the width of EDC's, the gap magnitude (Δ) is approximately given by 2–3 times Δ_{LEM} [12]. As shown in Fig. 2(b), a relationship $\Delta = 2.2\Delta_{\text{LEM}}$ well explains both the LEM and peak shift in the $x = 0.15$ data and also explains the data for $x = 0.03$ and 0.07 . Therefore, we have assumed this relationship for analysis of the Δ^* and Δ_0 as described below.

In Fig. 2(c), the doping dependence of the observed Δ^* and Δ_0 thus deduced are summarized. The doping dependence of Δ^* is quantitatively consistent with various spectroscopic data such as B_{1g} -geometry Raman scattering [9]. $\Delta^* \sim 30$ meV for the $x = 0.15$ sample is consistent with the previous ARPES results, too [14]. On the other hand, Δ_0 remains unchanged in going from $x = 0.15$ to $x = 0.07$ and vanishes in the nonsuperconducting sample $x = 0.03$ [21], similar to the results of the lightly doped Bi2212 [10]. However, vortex-liquid states suggestive of superconducting states were observed in $x = 0.03$ [22]. The present result $\Delta_0 \sim 0$ for $x = 0.03$ may be due to the high tem-

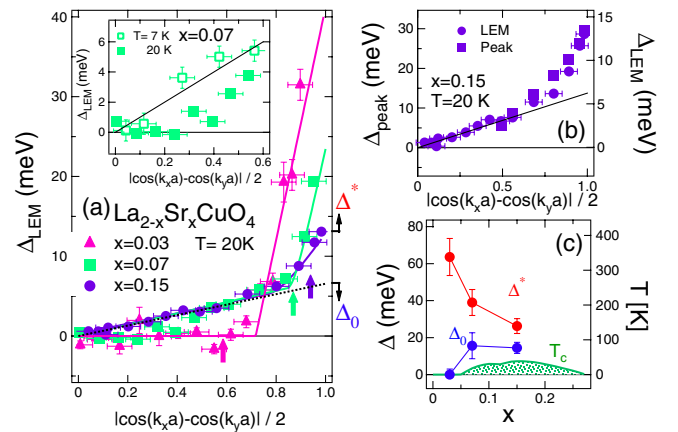


FIG. 2 (color online). Momentum dependence of the energy gap at $T = 20$ K in LSCO with various doping levels. (a): Leading edge midpoints (LEM) Δ_{LEM} relative to that at the node. Vertical arrows represents the boundary of the AFM BZ. Inset shows LEM near the node for $x = 0.07$ below and above T_c ($=14$ K). (b): Comparison of the peak position (Δ_{peak}) and Δ_{LEM} for $x = 0.15$, indicating the relationship $\Delta_{\text{peak}} \cong 2.2\Delta_{\text{LEM}}$. (c): Doping dependence of Δ^* and Δ_0 obtained by assuming the relation in panel (b).

perature effects similar to the LEM above T_c near the nodal direction for $x = 0.07$.

The temperature dependence of the gap is shown in Fig. 3. In Figs. 3(a1), 3(a2), 3(a3), and 3(a4), EDC's for $x = 0.15$ exhibit clear shifts of the LEM between the nodal and antinodal directions in the $T = 20, 55$ and 80 K data. In contrast, the LEM at $T = 155$ K show almost no shift between the nodal and antinodal direction, indicating that the gap is closed on the entire Fermi surface. The angular dependence of the Δ_{LEM} for each temperature are plotted in Fig. 3(b). As shown in the inset, Δ^* decreases with increasing temperature and closes at $T^* \sim 150$ K, again consistent with T^* obtained from the angle-integrated photoemission results [15]. Δ_0 also decreases with temperature similar to the decrease of T_c . However Δ_0 seems finite at $T = 55$ K, slightly above T_c . Probably, the gap closes near the node direction [19], although the low energy scales in LSCO did not allow us to resolve it.

Now, let us compare the two-gap energy scales of LSCO with those of other high- T_c cuprates to clarify their relation to T_c . In Fig. 4(a), the doping dependences of Δ^* , Δ_0 and T^* for LSCO and another single-layer cuprate Bi2201 are plotted. In the same manner, those for double-layer Bi2212 which has about twice higher T_c than those of LSCO are plotted in Fig. 4(b). Interestingly, the doping dependences of Δ^* of all these samples approximately scale with T^* following the relationship $2\Delta^*/k_B T^* = 4.3$, reminiscent of the d -wave BCS relationship [23]. Furthermore, these data fall on approximately the same lines for all the compounds irrespective of the different T_c as indicated in Figs. 4(a) and 4(b). Especially, pseudogap temperatures for optimally doped $\text{Bi}_2\text{Sr}_2\text{Ca}_2\text{Cu}_3\text{O}_{10}$ (Bi2223) [24] and Bi2201 [12]

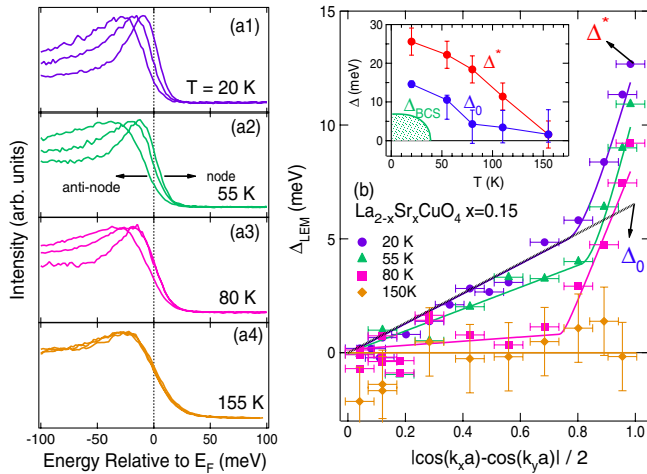


FIG. 3 (color online). Momentum dependence of the energy gap for $x = 0.15$ at various temperatures. (a1)–(a4): EDC's at k_F in the nodal to the antinodal directions. (b): Momentum dependence of Δ_{LEM} along the Fermi surface for $x = 0.15$ at various temperatures. Inset shows the temperature dependence of Δ^* and Δ_0 with the assumption $\Delta = 2.2\Delta_{\text{LEM}}$, as in Fig. 2. The d -wave BCS gap Δ_{BCS} ($=4.3k_B T_c/2$) is also plotted for comparison.

are both $T^* \sim 150$ K, similar to the present result of LSCO $T^* \sim 140$ K, although they have very different T_c 's. Therefore, we speculate that Δ^* is a universal property of a single CuO_2 plane and is not much affected by its chemical environment [25]. One possible explanation for the material independence of Δ^* is that its magnitude is determined by J , since the exchange interaction J is almost material independent. A pseudogap originated from anti-ferromagnetic spin fluctuations [26] or RVB-type spin singlet formation [27] has its origin in J . Indeed, a phenomenological model where the pseudogap Δ^* comes from the RVB gap explains the two characteristic gap energy scales [28,29].

In contrast to Δ^* , the d -wave order parameter Δ_0 of Bi2212 is twice as large as those of LSCO, reminiscent of the difference in the magnitude of T_c . The strong material dependences of Δ_0 mean that Δ_0 is not a property only of a single CuO_2 plane but also influenced by the environment such as the apical oxygens or the block layers and/or the neighboring CuO_2 planes in multilayer cuprates. Namely, the number of CuO_2 layers and the distance of the apical oxygen atoms (in block layers) from the CuO_2 plane are important factors for the superconducting gap and hence T_c . The effect from outside the CuO_2 plane has been modelled using the distant-neighbor hopping parameters t' and t'' [30], which are affected by the p_z orbital of the apical oxygen and the position of the empty Cu $4s$ orbital. In other words, the $(\pi, 0)$ pseudogap does not depend on details of the band structure nor on the parameters t' , t'' , but only on t and/or J .

If the pseudogap in the antinodal region precludes contribution to the superconductivity and the superconductivity comes mainly from the near-nodal region, the “effective” superconducting gap $\Delta_{\text{sc}} \propto (\text{Fermi arc length}) \times \Delta_0$ rather than Δ_0 would be more directly related to T_c [31]. Here, the Fermi arc is defined by the momentum region

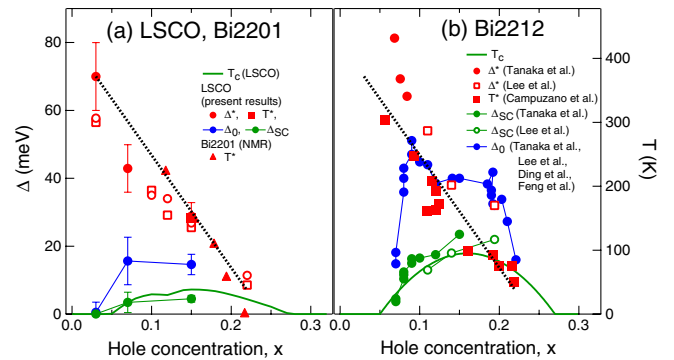


FIG. 4 (color online). Doping dependence of the characteristic energies (Δ^* , Δ_0) and temperatures (T^* , T_c) for single-layer cuprates (LSCO, Bi2201) (a) and double-layer cuprates Bi2212 (b). Gap energies Δ and temperatures T have been scaled as $2\Delta = 4.3k_B T$ in both panels. Parameter values have been taken from NMR results for Bi2201 [33], and ARPES for Bi2212 [4,10,11,34,35].

where the energy gap closes just above T_c . According to the high-resolution ARPES, the arc length for LSCO ($x = 0.15$) is $\sim 30\%$ of the entire Fermi surface [14]. For $x = 0.07$, the arc length is $\sim 20\%$ as seen in the inset of Fig. 2. Using these value for LSCO, the doping dependence of $\Delta_{sc} = (\text{arc length}) \times \Delta_0$ is plotted in Fig. 4(a). In the same manner, Δ_{sc} for Bi2212 were determined by using the Fermi arc length [11] [Fig. 4(b)]. The plotted Δ_{sc} approximately agree with the dome of T_c through the BCS formula $2\Delta_{sc} = 4.3k_B T_c$. Particularly, the decrease of T_c with underdoping can be ascribed to the reduction of the Fermi arc length together with the Δ_0 , which remains nearly constant till $x \sim 0.07$ and then drops. As for the nonsuperconducting $x = 0.03$ sample, the arc length may be too short to produce sufficient carriers for superconductivity or the nodal spectra may have a small gap due to localization as seen in the transport properties [32].

In summary, we have reported an ARPES result of LSCO and have clearly shown a signature of the two distinct energy gap scales, Δ^* and Δ_0 . From comparison of the present results with those of other cuprates, we have found that the magnitude of Δ^* is almost material independent, suggesting that the pseudogap is a distinct phenomenon from superconductivity. On the other hand, Δ_0 exhibits a large difference between materials, reflecting the different superconducting properties including the different T_c 's. Using the obtained two-gap parameters in conjunction with the Fermi arc picture [31], we have obtained the magnitude of the “effective” superconducting gap and consistently explained the doping dependence of T_c in LSCO as well as in Bi2212. The present results enforce the picture of superconductivity on the Fermi arc and clarify how T_c disappears in the underdoped region. Since the observed material dependence of Δ_0 is a crucial factor for the high- T_c superconductivity, the relationship between Δ_0 and other model parameters such as t' and t'' , the number of CuO_2 planes, the apical oxygen—Cu distance, and possibly electron-phonon coupling, has to be clarified in future studies.

We are grateful to C. M. Ho, M. Ido, G.-q. Zheng, and C. Panagopoulos for enlightening discussions. This work was supported by a Grant-in-Aid for Scientific Research in Priority Area “Invention of Anomalous Quantum Materials”, Grant-in-Aid for Young Scientists from the Ministry of Education, Science, Culture, Sports and Technology and the U.S. DOE Contract DE-FG03-01ER45876 and DE-AC03-76SF00098. Y.A. was supported by KAKENHI 19674002 and 20030004. ALS is operated by the Department of Energy's Office of Basic Energy Science, Division of Materials Science.

Experiment at the Photon Factory was approved by the Photon Factory Program Advisory Committee (Proposal No. 2006S2-001).

-
- [1] J. V. Emery and S. A. Kivelson, *Nature (London)* **374**, 434 (1995).
 - [2] J. R. Engelbrecht, A. Nazarenko, M. Randeria, and E. Dagotto, *Phys. Rev. B* **57**, 13 406 (1998).
 - [3] S. Chakravarty, R. B. Laughlin, Dirk K. Morr, and C. Nayak, *Phys. Rev. B* **63**, 094503 (2001).
 - [4] J. C. Campuzano *et al.*, *Phys. Rev. Lett.* **83**, 3709 (1999).
 - [5] N. Miyakawa *et al.*, *Phys. Rev. Lett.* **80**, 157 (1998).
 - [6] G. Deutscher, *Nature (London)* **397**, 410 (1999).
 - [7] C. Panagopoulos, J. R. Cooper, and T. Xiang, *Phys. Rev. B* **57**, 13 422 (1998).
 - [8] M. Opel *et al.*, *Phys. Rev. B* **61**, 9752 (2000).
 - [9] M. Le Tacon *et al.*, *Nature Phys.* **2**, 537 (2006).
 - [10] K. Tanaka *et al.*, *Science* **314**, 1910 (2006).
 - [11] W. S. Lee *et al.*, *Nature (London)* **450**, 81 (2007).
 - [12] T. Kondo *et al.*, *Phys. Rev. Lett.* **98**, 267004 (2007).
 - [13] M. Hashimoto *et al.*, *Phys. Rev. B* **79**, 144517 (2009).
 - [14] K. Terashima *et al.*, *Phys. Rev. Lett.* **99**, 017003 (2007).
 - [15] M. Hashimoto *et al.*, *Phys. Rev. B* **75**, 140503(R) (2007).
 - [16] M. R. Norman *et al.*, *Phys. Rev. B* **76**, 174501 (2007).
 - [17] T. Valla *et al.*, *Science* **314**, 1914 (2006).
 - [18] A. Kanigel *et al.*, *Nature Phys.* **2**, 447 (2006).
 - [19] J. Meng *et al.*, *Phys. Rev. B* **79**, 024514 (2009).
 - [20] T. Yoshida *et al.*, *Phys. Rev. B* **63**, 220501(R) (2001).
 - [21] For $x = 0.03$, although $\Delta_{\text{LEM}} \sim 0$ on most of the Fermi surface, spectral weight is appreciable only near the node, yielding the short Fermi arc.
 - [22] L. Li *et al.*, *Nature Phys.* **3**, 311 (2007).
 - [23] H. Won and K. Maki, *Phys. Rev. B* **49**, 1397 (1994).
 - [24] T. Sato *et al.*, *Phys. Rev. Lett.* **89**, 067005 (2002).
 - [25] Disorder has been shown to influence T^* to some extent. [Okada *et al.*, *J. Phys. Chem. Solids* **69**, 2989 (2008); *J. Phys. Soc. Jpn.* **77**, 074714 (2008)].
 - [26] P. Prelovsek and A. Ramsak, *Phys. Rev. B* **65**, 174529 (2002).
 - [27] H. Fukuyama and H. Kohno, in *Physics and Chemistry of Transition-Metal Oxides*, edited by H. Fukuyama and N. Nagaosa (Springer, Berlin, 1999), p. 231.
 - [28] K. Y. Yang, T. M. Rice, and F. C. Zhang, *Phys. Rev. B* **73**, 174501 (2006).
 - [29] K. Y. Yang *et al.*, *Europhys. Lett.* **86**, 37002 (2009).
 - [30] E. Pavarini *et al.*, *Phys. Rev. Lett.* **87**, 047003 (2001).
 - [31] M. Oda, R. M. Distasupil, N. Momono, and M. Ido, *J. Phys. Soc. Jpn.* **69**, 983 (2000).
 - [32] Y. Ando *et al.*, *Phys. Rev. Lett.* **87**, 017001 (2001).
 - [33] G. q. Zheng *et al.*, *Phys. Rev. Lett.* **94**, 047006 (2005).
 - [34] H. Ding *et al.*, *Phys. Rev. Lett.* **87**, 227001 (2001).
 - [35] D. L. Feng *et al.*, *Phys. Rev. Lett.* **86**, 5550 (2001).